

# A Novel Multi Input DC-DC Converter for Integrated Wind, PV Renewable Energy Generated System

S.Ramya<sup>1</sup>, T.Manokaran<sup>2</sup>

<sup>1</sup>P.G Scholar, Department of Electronic and Communication Engineering, V.S.B Engineering College, Karur, India

<sup>2</sup>Associate Professor, Department of Electrical and Electronics Engineering, Sri Subramanya College of Engineering and Technology, Sukkamaikanpatti, Palani, Dindigul, India

---

**Abstract:**—The objective of this paper is to propose a novel multi-input power converter for the grid-connected hybrid renewable energy system in order to simplify the power system and reduce the cost. The proposed multi-input power converter consists of a Cuk fused multi-input dc-dc converter and a full-bridge dc-ac inverter. The incremental conductance method is mainly used to accomplish the maximum power point tracking (MPPT) algorithm for input sources. The operational principle of the proposed multi-input power converter is explained. A multi-input power converter (MIPC) which operates in four modes: first an operation type wherein power is delivered to dc Bus from hybrid renewable energy sources; second a single type wherein only one renewable energy source supplies power to the dc Bus; third an inverter type wherein power is delivered to dc Bus from ac grid via inverter module, and fourth a battery type wherein power is delivered to dc Bus from batteries without renewable energy source. The integration of the dc Bus and a hybrid renewable power supply system is implemented and simulated using MATLAB/SIMULINK. A hybrid renewable power energy which integrates the solar energy, wind-power.

**Keywords:**—Inverter, Photo Voltaic (PV), Wind Energy, MIPC, CUK, IncCond, Renewable Energy System, DC bus.

---

## I. INTRODUCTION

Based on conventional sources of energy are rapidly depleting and the cost of energy is rising, photovoltaic and wind energy becomes a promising alternative source. Among its advantages are that it is: 1) abundant; 2) pollution free; 3) distributed throughout the earth; and 4) recyclable. The main drawbacks are that the initial installation cost is considerably high and the energy conversion efficiency is relatively low. To overcome these problems, the following two essential ways can be used: 1) increase the efficiency of conversion and 2) maximize the output power. With the development of technology, the cost of the solar arrays and wind turbines is expected to decrease continuously in the future, making them attractive for residential and industrial applications. Various methods of maximum power tracking have been considered in photovoltaic power applications [1]–[8]. Of these, the incremental conductance (IncCond), which moves the operating point toward the maximum power point by periodically increasing or decreasing the array voltage, is often used in many photovoltaic systems [3]–[6]. The incremental conductance method (IncCond) is also now often used in photovoltaic systems [7], [8]. The IncCond method quickly tracks the maximum power points by comparing the incremental and instantaneous conductance's of the solar array. The incremental conductance is estimated by measuring small changes in array voltage and current. These small changes may be induced by deliberate control action. Methods which improve the IncCond method and can identify the incremental conductance of the array are now more rapidly have been proposed [9]. However, the harmonic components of the array voltage and current need to be measured and it is used to adjust the array reference voltage. The objective of this paper is to propose a novel multi-input power converter for grid-connected hybrid renewable system. The proposed multi-input power converter system has three advantages: i) power from the PV and the wind turbine can be delivered to the utility grid individually or simultaneously, ii) maximum power point tracking feature is realized for both solar and wind energy, and iii) a wide range of input voltage variation is caused by different insulation and wind speed is acceptable.

## II. PRINCIPLE OF THE PROPOSED MULTI-INPUT POWER CONVERTER

The circuit diagram of the proposed multi-input power converter is shown in Fig. 2. It consists of a Cuk fused multi-input dc-dc converter and a full-bridge dc/ac inverter. The input dc voltage sources,  $V_{pv}$  and  $V_{wind}$ , are obtained from the PV array and the rectified wind turbine output voltage. By applying the pulse-width modulation (PWM) control scheme with appropriate MPPT algorithm to the power switches M1 and M2, the multi-input dc-dc converter can draw maximum power from both the PV array and the wind turbine individually or simultaneously. The dc bus voltage  $V_{DC}$ , will be regulated by the dc/ac inverter with sinusoidal PWM (SPWM) control to achieve the input output power-flow balance. Details of the operation principle for the proposed multi-input inverter are introduced as follows.

### 1. PV Array:

The PV array is constructed by many series or parallel connected solar cells [10]. Each solar cell is formed by a P-N junction semiconductor, which can produce currents by the photovoltaic effect. It can be seen that a maximum power point exists on each output power characteristic curve. Therefore, to utilize the maximum output power from the PV array, an appropriate control algorithm must be adopted.

**2. MPPT Algorithm:**

Different MPPT techniques have been developed. Among these techniques, the incremental conductance (IncCond) method with the merit of simplicity is used in this paper. The perturbation of the output power is achieved by periodically changing (either increasing or decreasing) the controlled output current. The objective of the IncCond method is to determine the changing direction of the load current. Fig. 1 shows the flow chart of the MPPT algorithm with IncCond method for the proposed multi-input inverter. Since there are two individual input sources, each one of them needs an independent controller. However, both of the controllers can be implemented by using one integrated controller. At the beginning of the control scheme, the output voltage and output current of the source (either the PV array or the wind turbine) are measured, then the output power can be calculated. On comparing the recent values of power, current and voltage with previous method, the IncCond method shown in the flow chart can determine the value of reference current to adjust the output power toward the maximum point. [11]

**3. Wind Energy Generating System:**

The induction generator is used in the proposed scheme because of its simplicity, it does not require a separate field circuit, it can accept constant and variable loads, and has natural protection against short circuit. The available power of wind energy system is presented as under in Eq. 1.

$$P_{wind} = \frac{1}{2} \rho A V_{wind}^3 \tag{1}$$

Where  $(\text{kg/m}^3)$  is the air density and  $A \text{ (m}^2\text{)}$  is the area swept out by turbine blade,  $V_{wind}$  is the wind speed in mtr/s. It is not possible to extract all the kinetic energy of wind, but it extracts a fraction of power in wind, which we call power coefficient  $C_p$  of the wind turbine, and is given in Eq. 2.

$$P_{mech} = C_p P_{wind} \tag{2}$$

Where  $C_p$  is the power coefficient, depends on operating condition of wind turbine. This coefficient can be expressed as a function of tip speed ratio  $\lambda$  and pitch angle  $\theta$ . The mechanical power produced by wind turbine is given in Eq. 3.

$$P_{mech} = \frac{1}{2} \rho \pi R^2 V_{wind}^3 C_p \tag{3}$$

Where  $R$  is the radius of the wind blade (m).

**4. Multi-Input DC-DC Converter:**

The proposed multi-input dc-dc converter is the fusion of the Cuk converter [12]. Syntheses of the multi input dc-dc converter are done by inserting the pulsating voltage source of the buck-boost converter into the Cuk

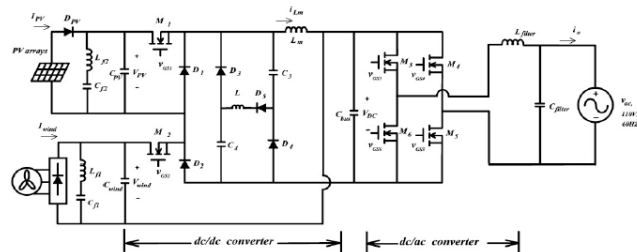


**Fig.1** Schematic diagram of the proposed multi-input inverter.

converter. In order not to hamper the normal operation of the buck-boost converter and to utilize the inductor for the Cuk converter, the pulsating voltage source of the Cuk converter must be series connected with the output inductor. Fig. 3 presents the configuration of the proposed hybrid renewable energy generation with multi-input power converter for dc bus [13]. The generation subsystems comprise a wind turbine (WT) generator, a PV, two HCPVs including active sun tracker, and a battery bank (BT). The multiinput power converter comprises WT modules, PV modules, HCPV modules, hydraulic generator module [14] in expectation, an inverter (IT) module, a control module, and a BT module, in which the dc power was charged for storing energy.

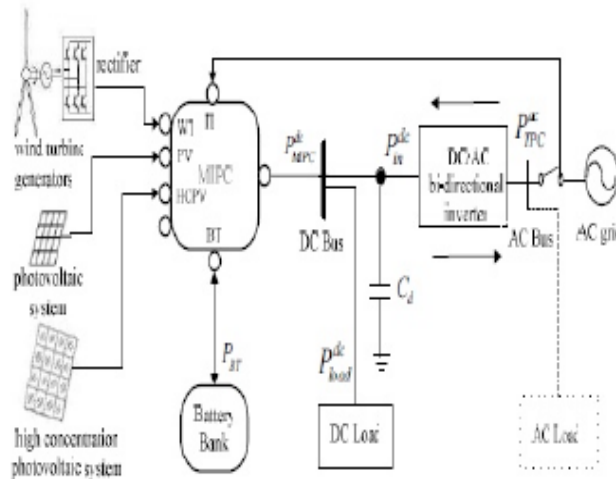


**Fig. 2** Configuration of the hybrid power generation with multi-input power converter.

### III. CONVERTER STRUCTURE AND OPERATION MODES

The structure of the proposed three-input dc–dc boost converter is represented in **Fig. 2**. As seen from the figure, the converter interfaces two input power sources  $v_1$  and  $v_2$ , and a battery as the storage element. The proposed converter is suitable alternative for hybrid power systems of PV, FC, and wind sources. Therefore,  $v_1$  and  $v_2$  are shown as two dependent power sources that their output characteristics are determined by the type of input power sources. For example, for a PV source at the first port,  $v_1$  is identified as a function of its current  $i_{L1}$ , light intensity, and ambient temperature. In the converter structure, two inductors  $L_1$  and  $L_2$  make the input power ports as two current-type sources, which result in drawing smooth dc currents from the input power sources. The  $RL$  is the load resistance, which can represent the equivalent power feeding an inverter. Four power switches  $S_1, S_2, S_3$ , and  $S_4$  in the converter structure are the main controllable elements that control the power flow of the hybrid power system. The circuit topology enables the switches to be independently controlled through four independent duty ratios  $d_1, d_2, d_3$ , and  $d_4$ , respectively. As like as the conventional boost converters, diodes  $D_1$  and  $D_2$  conduct incomplementary manner with switches  $S_1$  and  $S_2$ . The converter structure shows that when switches  $S_3$  and  $S_4$  are turned ON, their corresponding diodes  $D_3$  and  $D_4$  are reversely biased by the battery voltage and then blocked. On the other hand, turn OFF state of these switches makes diodes  $D_3$  and  $D_4$  able to conduct input currents  $i_{L1}$  and  $i_{L2}$ . In hybrid power system applications, the input power sources should be exploited in continuous current mode (CCM). For example, in the PV or FC systems, an important goal is to reach an acceptable current ripple in order to set their output power on desired value. Therefore, the current ripple of the input sources should be minimized to make an exact power balance among the input powers and the load. Therefore, in this paper, steady state and dynamic behavior of the converter have been investigated in CCM.

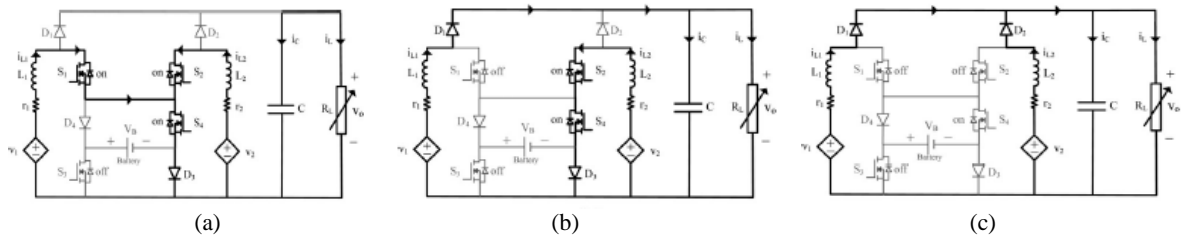


**Fig. 3.** First operation mode. (a) Switching state 1:  $0 < t < d_1 T$ . (b) Switching state 2:  $d_1 T < t < d_2 T$ . (c) Switching state 3:  $d_2 T < t < T$ .

In general, depending on utilization state of the battery, three power operation modes are defined to the proposed converter. These modes of operation are investigated with the assumptions of utilizing the same sawtooth carrier waveform for all the switches, and  $d_3, d_4 < \min(d_1, d_2)$  in battery charge or discharge mode. Although exceeding duty ratios  $d_3$  and  $d_4$  from  $d_1$  or  $d_2$  does not cause converter malfunction, it results in setting the battery power on the possible maximum values. In order to simplify the investigations, it is assumed that duty ratio  $d_1$  is less than duty ratio  $d_2$ . Further, with the assumption of ideal switches, the steady-state equations are obtained in each operation mode.

#### 1. First Power Operation Mode (Supplying the Load With Sources $v_1$ and $v_2$ Without Battery Existence):

In this operation mode, two input power sources  $v_1$  and  $v_2$  are responsible for supplying the load, and battery charging/ discharging is not done. This operation mode is considered as the basic operation mode of the converter. As clearly seen from the converter structure, there are two options to conduct input power sources currents  $i_{L1}$  and  $i_{L2}$  without passing through the battery; path 1:  $S_4-D_3$ , path 2:  $S_3-D_4$ . In this operation mode, the first path is chosen; therefore, switch  $S_3$  is turned OFF while switch  $S_4$  is turned ON entirely in the switching period ( $d_4 = 1$  and  $d_3 = 0$ ). Thus, three different switching states of the converter are achieved in one switching period. These switching states are depicted in Fig. 3(a)–(c). Also, the steady-state waveforms of the gate signals of the four switches and the variations of inductors currents  $i_{L1}$  and  $i_{L2}$ .

**Switching state 1** ( $0 < t < d_1 T$ ): At  $t = 0$ , switches  $S_1$  and  $S_2$  are turned ON and inductors  $L_1$  and  $L_2$  are charged with voltages across  $v_1$  and  $v_2$ , respectively.

**Switching state 2** ( $d_1 T < t < d_2 T$ ): At  $t = d_1 T$ , switch  $S_1$  is turned OFF, while switch  $S_2$  is still ON (according to the assumption  $d_1 < d_2$ ). Therefore, inductor  $L_1$  is discharged with voltage across  $v_1 - v_0$  into the output load and the capacitor through diode  $D_1$ , while inductor  $L_2$  is still charged by voltage across  $v_2$ .

**Switching state 3** ( $d_2 T < t < T$ ): At  $t = d_2 T$ , switch  $S_2$  is also turned OFF and inductor  $L_2$  is discharged with voltage across  $v_2 - v_0$ , as like as inductor  $L_1$ . By applying voltage-second and current-second balance theory to the converter, following equations are obtained.

$$L_1: d_1 T(v_1 - r_1 i_{L1}) + (1 - d_1)T(v_1 - r_1 i_{L1} - v_0) = 0 \rightarrow v_0 = \frac{v_1 - r_1 i_{L1}}{1 - d_1} \quad (4)$$

$$L_2: d_2 T(v_2 - r_2 i_{L2}) + (1 - d_2)T(v_2 - r_2 i_{L2} - v_0) = 0 \rightarrow v_0 = \frac{v_2 - r_2 i_{L2}}{1 - d_2} \quad (5)$$

$$C: (1 - d_1)T i_{L1} + (1 - d_2)T i_{L2} = T \frac{v_0}{R_L} \quad (6)$$

$$i_{batt} = 0 \rightarrow P_{batt} = 0 \quad (7)$$

In this operation mode, the control strategy is based on regulating one of the input sources on its reference power with its corresponding duty ratio, while the other power source is utilized to regulate the output voltage by means of its duty ratio.

## 2. Second Power Operation Mode (Supplying the Load with Sources $v_1$ and $v_2$ and the Battery):

In this operation mode, two input power sources  $v_1$  and  $v_2$  along with the battery are responsible for supplying the load. Therefore, discharging state of the battery should be provided in this operation mode. Referring to the converter topology, when switches  $S_3$  and  $S_4$  are turned ON simultaneously, currents  $i_{L1}$  and  $i_{L2}$  are conducted through the path of switch  $S_4$ , the battery, and switch  $S_3$  which results in battery discharging. However, discharging operations of the battery can only last until switches  $S_1$  and/or  $S_2$  are conducting. As a result, the maximum discharge power of the battery depends on duty ratios of  $d_1$  and  $d_2$  as well as currents  $i_{L1}$  and  $i_{L2}$ .

$$P_{bat.dis}^{max} = v_B [d_1 i_{L1} + d_2 i_{L2}], \quad S_3=ON, S_4=ON \quad (8)$$

Therefore, in order to acquire a desired maximum discharging power of the battery, the input power sources should be designed in proper current and voltage values. On the other hand, regulating the discharging power of the battery below  $P_{maxbat.dis}$  can be made by changing the state of only one of switches  $S_3$  and  $S_4$  before switches  $S_1$  and  $S_2$  are turned OFF (according to the assumption  $d_3, d_4 < \min(d_1, d_2)$ ). In this paper, duty ratio  $d_4$  is controlled to regulate the discharging power of the battery regarding the facts that when  $S_4$  is turned ON, it results in passing the currents of input power sources through the battery; hence, the battery discharge mode is started, and its turn-OFF state starts conducting through diode  $D_4$  and stops discharging the battery.

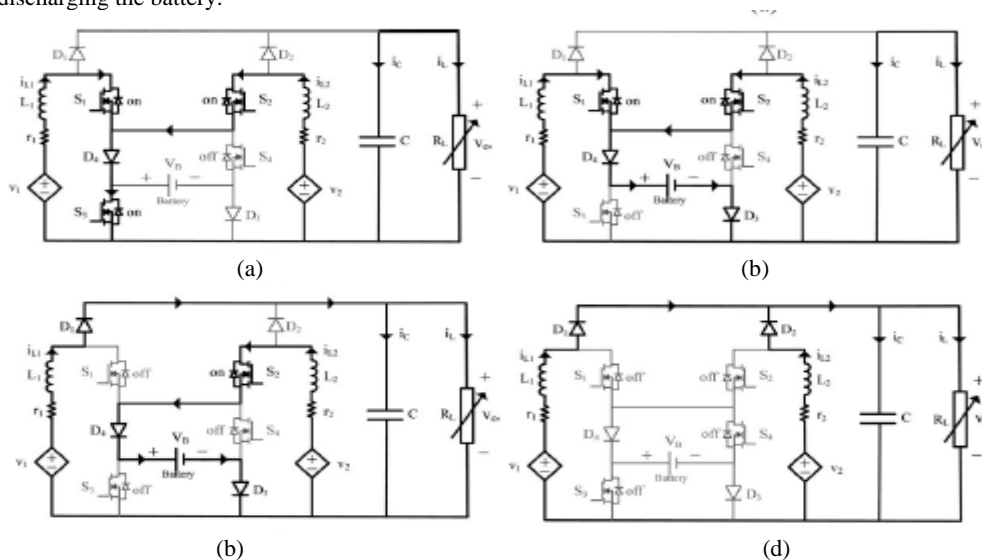


**Fig. 4** Second operation mode. (a) Switching state 1:  $0 < t < d_4 T$ . (b) Switching state 2:  $d_4 T < t < d_1 T$ . (c) Switching state 3:  $d_1 T < t < d_2 T$ . (d) Switching state 4:  $d_2 T < t < T$ .

As depicted in Fig. 4(a)–(d), there are four different switching states for the converter in one switching period. The steady-state waveforms of the gate signals of the four switches and the variations of input currents  $i_{L1}$  and  $i_{L2}$ .

**Switching state 1** ( $0 < t < d_4 T$ ): At  $t = 0$ , switches  $S_1$ ,

$S_2$ , and  $S_4$  are turned ON, so inductors  $L_1$  and  $L_2$  are charged with voltages across  $v_1 + v_B$  and  $v_2 + v_B$ , respectively [Fig. 4(a)].

**Switching state 2** ( $d_4 T < t < d_1 T$ ): At  $t = d_4 T$ , switch  $S_4$  is turned OFF, while switches  $S_1$  and  $S_2$  are still ON. Therefore, inductors  $L_1$  and  $L_2$  are charged with voltages across  $v_1$  and  $v_2$ , respectively [Fig. 4(b)].

**Switching state 3** ( $d_1 T < t < d_2 T$ ): At  $t = d_1 T$ , switch  $S_1$  is turned OFF, so inductor  $L_1$  is discharged with voltage across  $v_1 - v_0$ , while inductor  $L_2$  is still charged with voltages across  $v_2$  [Fig. 4(c)].

**Switching state 4** ( $d_2T < t < T$ ): At  $t = d_2T$ , switch  $S_2$  is also turned OFF and inductors  $L_1$  and  $L_2$  are discharged with voltage across  $v_1 - v_o$  and  $v_2 - v_o$ , respectively. By applying voltage-second and current-second balance theory to the converter, following equations are obtained [Fig. 4(d)].

$$L_1: d_4T(v_1 - r_1iL_1 + v_B) + (d_1 - d_4)T(v_1 - r_1iL_1) + (1 - d_1)T(v_1 - r_1iL_1 - v_o) = 0$$

$$\rightarrow v_o = \frac{v_1 - r_1iL_1 + d_4v_B}{1 - d_1} \quad (9)$$

$$L_2: d_4T(v_2 - r_2iL_2 + v_B) + (d_2 - d_4)T(v_2 - r_2iL_2) + (1 - d_2)T(v_2 - r_2iL_2 - v_o) = 0 \rightarrow v_o = \frac{v_2 - r_2iL_2 + d_4v_B}{1 - d_2} \quad (10)$$

$$C: (1 - d_1)TiL_1 + (1 - d_2)TiL_2$$

$$= T \frac{v_o}{R_L} \quad (11) \text{Battery} \begin{cases} i_{Batt} = d_4(iL_1 + iL_2) \\ P_{Batt} = v_B[d_4(iL_1 + iL_2)] \end{cases} \quad (12)$$

In this operation mode, the control strategy is based on regulating both of the input power sources on their reference power by means of their corresponding duty ratios  $d_1$  and  $d_2$ , while the battery discharge power is utilized to regulate the output voltage by duty ratio  $d_4$ .

**3. Third Power Operation Mode (Supplying the Load With Sources  $v_1$  and  $v_2$ , and Battery Charging Performance):**

In this operation mode, two input power sources  $v_1$  and  $v_2$  are responsible for supplying the load while the battery charging performance is accomplished. Therefore, the charging state of the battery should be provided in this operation mode. Referring to the converter topology, when switches  $S_3$  and  $S_4$  are turned OFF, by turning ON switches  $S_1$  and  $S_2$ , currents  $iL_1$  and  $iL_2$  are conducted through the path of diode  $D_4$ , the battery, and diode  $D_3$ ; therefore, the condition of battery charging is provided. However, the charging operation of the battery can only last until switches  $S_1$  and/or  $S_2$  are conducting. As a result, the maximum charge power of the battery depends on duty ratios  $d_1$  and  $d_2$  as well as currents  $iL_1$  and  $iL_2$ .

$$P_{bat.dis}^{max} = v_B[d_1iL_1 + d_2iL_2], \quad S_3=OFF, S_4=OFF \quad (13)$$

Therefore, in order to acquire a desired maximum charge power of the battery, the input power sources should be designed in proper current and voltage values. On the other hand, regulating the charging power of the battery below the  $P_{maxbat.ch}$  can be made by changing the state of only one of switches  $S_3$  and  $S_4$  before switches  $S_1$  and  $S_2$  are turned OFF (according to the assumption  $d_3, d_4 < \min(d_1, d_2)$ ). In this paper, in order to regulate the charging power of the battery, switch  $S_3$  is controlled by regarding the fact that when switch  $S_3$  is turned ON, the charging power of the battery is not accomplished while its turn-OFF state makes the battery to be charged with currents  $iL_1$

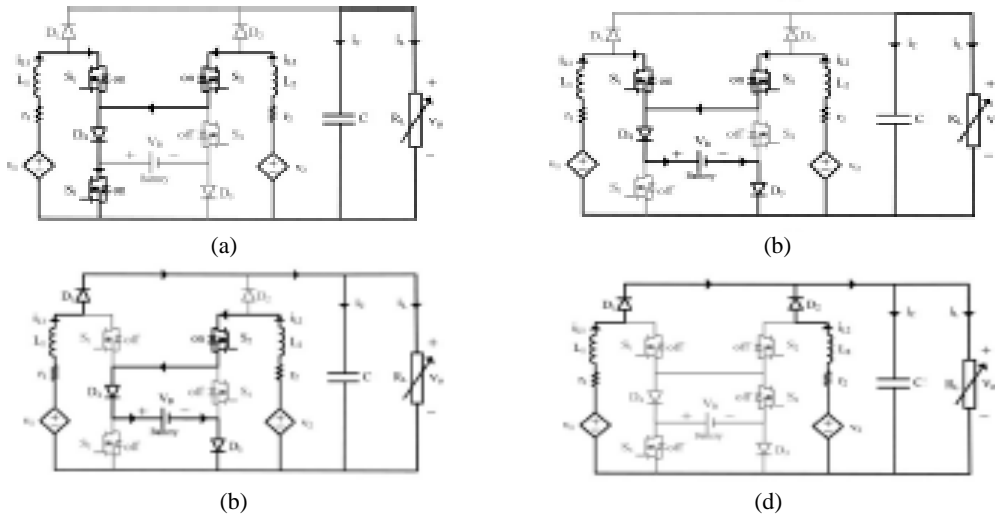


**Fig. 5.** Third operation mode. (a) Switching state 1:  $0 < t < d_3 T$ . (b) Switching state 2:  $d_3 T < t < d_1 T$ . (c) Switching state 3:  $d_1 T < t < d_2 T$ . (d) Switching state 4:  $d_2 T < t < T$ .

and  $iL_2$  through the path of  $D_3$ . Four different switching states occurred in one switching period are illustrated in Fig. 5(a)–(d). Also, the steady-state waveforms of the gate signals of the four switches and the variations of input currents  $iL_1$  and  $iL_2$ .

**Switching state 1** ( $0 < t < d_3 T$ ): At  $t = 0$ , switches  $S_1, S_2$ , and  $S_3$  are turned ON, so inductors  $L_1$  and  $L_2$  are charged with voltages across  $v_1$  and  $v_2$ , respectively [see Fig. 5(a)].

**Switching state 2** ( $d_3 T < t < d_1 T$ ): At  $t = d_3 T$ , switch  $S_3$  is turned OFF while switches  $S_1$  and  $S_2$  are still ON (according to the assumption). Therefore, inductors  $L_1$  and  $L_2$  are charged with voltages across  $v_1 - v_B$  and  $v_2 - v_B$ , respectively.

**Switching state 3** ( $d_1 T < t < d_2 T$ ): At  $t = d_1 T$ , switch  $S_1$  is turned OFF, so inductor  $L_1$  is discharged with voltage across  $v_1 - v_o$ , while inductor  $L_2$  is still charged with voltage across  $v_2 - v_B$ .

**Switching state 4** ( $d_2 T < t < T$ ): At  $t = d_2 T$ , switch  $S_2$  is also turned OFF and inductor  $L_2$  as like as  $L_1$  is discharged with voltage across  $v_2 - v_o$ .

By applying voltage-second and current-second balance theory to the converter, following equations are obtained:

$$L_1: d_3T(v_1 - r_1iL_1) + (d_1 - d_3)T(v_1 - r_1iL_1 - v_B) + (1 - d_1)T(v_1 - r_1iL_1 - v_0) = 0 \rightarrow v_0$$

$$= \frac{v_1 - r_1iL_1 - (d_1 - d_3)v_B}{1 - d_1} \quad (13)$$

$$L_2: d_3T(v_2 - r_2iL_2) + (d_2 - d_3)T(v_2 - r_2iL_2 - v_B) + (1 - d_2)T(v_2 - r_2iL_2 - v_0) = 0 \rightarrow v_0$$

$$= \frac{v_2 - r_2iL_2 - (d_2 - d_3)v_B}{1 - d_2} \quad (14)$$

$$C: (1 - d_1)TiL_1 + (1 - d_2)TiL_2 = T \frac{v_0}{R_L} \quad (15)$$

In this operation mode, if the total generated power of the input sources becomes more than the load power, the battery charging performance will be possible if duty ratio  $d_3$  is utilized to regulate the output voltage. With this control strategy, duty ratios  $d_1$  and  $d_2$  are utilized to regulate powers of the input sources, while duty ratio  $d_3$  is utilized to regulate the output voltage through charging the battery by the extra-generated power. In all three operation modes, when one of the input power sources is not present to produce power, its corresponding duty ratio is set at zero, which results single power source operation for the converter.

#### IV. MODES OF PROPOSED MULTI-INPUT POWER

According to renewable energy sources provide power for the dc bus or the storage battery and where the battery bank absorbs the power to supply dc Bus, For the WT PV, and HCPV, supplying power for the dc bus via the MIPC is denoted by the “1”, otherwise by the “0”. For the storage battery bank, the “1” indicates a charge from MIPC, otherwise by the “0”. Moreover, for the power factor correction (PFC) mode of the inverter module connecting to the multi-power converter for supplying power is expressed by the “1”, else by the “0”. Therefore, we can use the bit-coding method to command or change the mode for the data patterns of typical digital signal processor (DSP) applications on data buses by MIPC. For example, consider the operation state from [11110] to [00011] that is the full mode of the operation type switching to the PFC mode of the inverter type in MIPC. Fig.4 shows the simplified sketch maps of the hybrid renewable energy distributed generation system under different operation modes by MIPC controller. Note that operation in each mode can be maintained as long as the battery bank energy is sufficient to satisfy the load requirements. If the high voltage dc Bus is under voltage low limit or over voltage high-limit, and then the output stage of MIPC is disconnected from the dc bus and avoids damages. At 3 this point in time, the hybrid renewable energy only export energy through the storage stage i.e. the power sources just charge up the storage battery. By following the above analytic approach, other operation modes also can be reduced.

#### V. CONTROL SCHEME

Conventional MPPT systems have two independent control loops to control MPPT. The first control loop contains the MPPT algorithm and the second one is usually a (proportional) P or (proportional and integral) PI controller. IncCond method makes use of instantaneous and incremental conductance to generate an error signal which is zero at MPP; however it is not zero at most of the operating points. The main purpose of the second control loop is to make the error from the MPPs near to zero [8]. Simplicity of operation, ease of design, inexpensive maintenance and low cost made PI controllers very popular in most linear systems. However, MPPT system of standalone photovoltaic (PV) and wind is a nonlinear control problem due to the nonlinearity nature of PV and unpredictable environmental conditions and hence PI controllers do not generally work well [15]. In this paper, the incremental conductance method with direct control is selected. The PI control loop is eliminated and duty cycle is adjusted directly in the algorithm. The control loop is simplified and the computational time for tuning controller gains is eliminated. To compensate the lack of PI controller in the proposed system a small marginal error of 0.002 was allowed. The objective of this work is to eliminate the second control loop and to show that sophisticated MPPT methods do not necessarily obtain the best results but employing them in simple manner for complicated electronic subjects is considered necessary. Feasibility of the proposed system is investigated with a DC-DC converter configured as the MPPT. In [16] it was mentioned that power extracted from PV modules with an analog circuitry can only operate at the MPP in a predefined illumination level.

#### VI. SIMULATION RESULTS

The proposed system is implemented and simulated using Matlab/Simulink that includes the PV module electrical circuit, Cuk converter and the MPPT algorithm. The PV module is modeled using electrical characteristics to provide output current and voltage of the PV module and wind turbine. The provided current and voltage are fed to the converter and the controllers simultaneously.

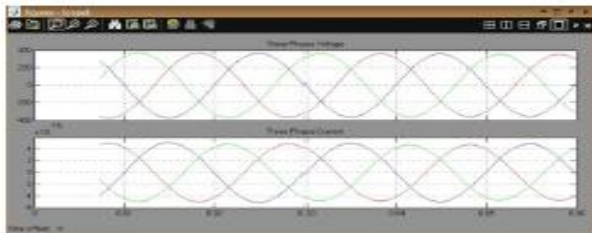


**Fig.6.** Wind Turbine Output Voltage and Current.



**Fig.7.** Converter Output Voltage.

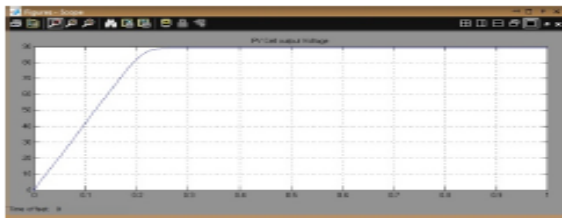


**Fig.8.**PV Output Voltage.

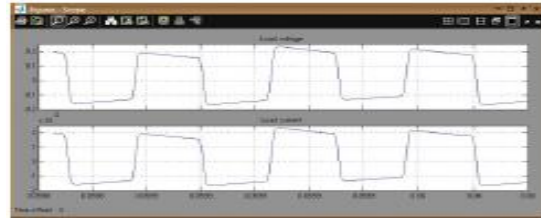


**Fig.9.**Load Voltage and Current.

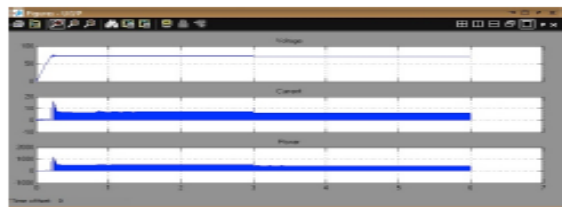


**Fig.10.**Output before Cuk converter.

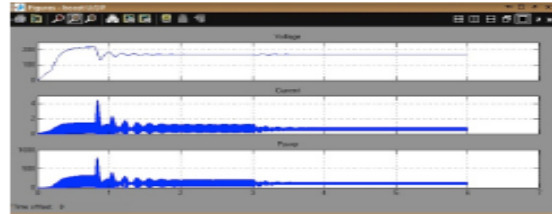


**Fig.11.**Output after Cuk converter

## VII. CONCLUSION

A novel multi-input power converter for the grid-connected hybrid renewable energy system is proposed. It has the following advantages: 1) power from the PV array or/and the wind turbine can be delivered to the utility grid individually or simultaneously, 2) MPPT feature is realized for both PV and wind energy, and 3) a large range of input voltage variation caused by different insulation and wind speed is made acceptable. In this paper, the operation principle of the proposed multi-input power converter has been introduced. Incremental conductance method is adopted to realize the MPPT algorithm for the PV array and the wind turbine. The control circuit is implemented and simulated by using MATLAB/SIMULINK. Simulation results at different operating conditions are shown here to verify the performance of the proposed multi-input power converter system with the desired features. From the results acquired during the simulation, it was confirmed that with a well-designed system including a proper converter and selecting an efficient proven algorithm, implementation of MPPT is simple and can be easily constructed to achieve an acceptable efficiency level of the PV modules and wind turbine.

## REFERENCES

- [1]. S. Rahmam, M. A. Khallat, and B. H. Chowdhury, "A discussion on the diversity in the applications of photovoltaic system," *IEEE Trans. Energy Conversion*, vol. 3, pp. 738–746, Dec. 1988.
- [2]. B. K. Bose, P. M. Szczesny, and R. L. Steigerwald, "Microcomputer control of a residential photovoltaic power conditioning system," *IEEE Trans. Ind. Applicat.*, vol. IA-21, pp. 1182–1191, Sept. 1985.
- [3]. B. H. Cho and P. Huynh, "Design and analysis of microprocessor controlled peak power tracking system," *Proc. 27th IECEC*, 1992, vol. 1, pp. 67–72.
- [4]. Wasynczuk, O., "Dynamic behaviour of a class of photo voltaic power systems," *IEEE Trans. Power App. Syst.*, vol. PAS-102, pp. 3031–3037, Sept. 1983.
- [5]. D. J. Caldwell *et al.*, "Advance space power system with optimized peak power tracking," *Proc. 26th IECEC*, 1991, vol. 2, pp. 145–150.
- [6]. L. Deheng and H. Yongji "A new method for optimal output of solar cell array," *Proc. IEEE Int. Symp. Industrial Electronics*, 1992, vol. 1, pp. 456–459.
- [7]. M. J. Powers and C. R. Sullivan, "A high efficiency mppt for photo voltaic array in a solar powered race vehicle," *Proc. IEEE PESC*, 1993, pp. 574–580.
- [8]. K. H. Hussein *et al.*, "Maximum photovoltaic power tracking: An algorithm for rapidly changing atmospheric conditions," *Proc. Inst. Elect. Eng.* vol. 142, pt. G, no. 1, pp. 59–64, Jan. 1995.
- [9]. S. Cuk and R. D. Middlebrook, "A general unified approach to modeling switching-converter power stages," *Proc. IEEE PESC*, 1976, pp. 18–34.
- [10]. D. B. Snyman and J. H. R. Enslin, "Combined low-cost, high-efficient inverter, peak power tracker and regulator for PV applications," *IEEE Tran. Power Electron.*, vol. 6, no. 1, pp. 73–82, Jan. 1991.
- [11]. Mekhilef S and Safari A, "Simulation and Hardware Implementation of Incremental Conductance MPPT with Direct Control Method Using Cuk Converter" *IEEE Trans. On Industrial Electronic*.
- [12]. Y.-C. Liu, Y.-M. Chen and S.-H. Lin, "Double-Input PWM DC/DC converter for high-low voltage sources," *Proc. IEEE Int. Telecommun. Energy Conf.*, 2003, pp. 27–32.
- [13]. T. C. Ou, C. L. Lee, and C. T. Lee, "DC Power Application with Hybrid Renewable Energy Resources for Intelligent," in *Proc. 29th Symp. Elect. Power Eng.*, Taiwan, Dec. 2008, pp. 1705–1710.
- [14]. X. J. Dai and F. T. Li, Q. Chao, "The research of wind power optimized capacity configuration of hydraulic power system," *Electric Utility Deregulation and Restructuring Power Technologies Third International Conference*, 6–9 Apr. 2008, pp. 2569–2574.
- [15]. Mohamed S. Adel Moteleb, Fawzan Salem, Hassan T. Dorrah, "An enhanced fuzzy and PI controller applied to MPPT problem" *Journal of Science and Engineering*, vol. 8, no. 2, pp. 147–153, 2005.
- [16]. A. Giustiniani, G. Petrone, M. Fortunato, G. Spagnuolo, M. Vitelli, "MPPT in a One-Cycle-Controlled Single-Stage Photovoltaic Inverter," *IEEE Trans. on Industrial Electronics*, vol. 55, no. 7, pp. 2684–2693, July 2008.